# Estimation of the Tritium Yields in Deuterium Fusion Plasmas Considering the Fast-Ion Velocity Distribution Function*)

Hideo NUGA[1)], Ryosuke SEKI[1,2)], Kunihiro OGAWA[1,2)], Shuji KAMIO[1)], Yutaka FUJIWARA[3)], Hiroyuki YAMAGUCHI[1,2)], Masaki OSAKABE[1,2)], Mitsutaka ISOBE[1,2)] and Masayuki YOKOYAMA[1,2)]

[1)]*National Institute for Fusion Science, National Institutes of Natural Sciences, Toki 509-5292, Japan*
[2)]*The Graduate University for Advanced Studies, SOKENDAI, Toki 509-5292, Japan*
[3)]*NTT Space Environment and Energy Laboratories, Tokyo 180-8585, Japan*

(Received 19 December 2021 / Accepted 12 February 2022)

Tritium yields due to the deuterium-deuterium fusion reaction during the 22nd LHD experiment campaign are numerically estimated. As usual, the total tritium yields are assumed to be the same total neutron yields. In the Large Helical Device (LHD), however, it is considered that fusion reactivity of the D(d,p)T branch is lower than that of the D(d,n)$^3$He one because the fusion reaction between a fast-deuteron and a thermal deuteron is dominant. By integrated simulation, considering the velocity distribution function of fast-deuteron, the ratio of the tritium yields to the neutron yields is estimated to be $Y_t/Y_n \sim 0.936$. From the assumptions applied in the simulation, it is expected that this value should be still an over-estimation rather than the actual value.



Keywords: LHD, deuterium experiment, neutron measurement, integrated simulation, tritium inventory

DOI: 10.1585/pfr.17.2402023

## 1. Introduction

In magnetically confined fusion devices using deuterium gas, a fusion reaction between deuterons (DD fusion) occurs. There are two branches of DD fusion. One emits a neutron and a $^3$He ion (D(d,n)$^3$He) and the other emits a tritium ion and a proton (D(d,p)T). Usually, it is regarded that these two reactions have the same reactivities. As shown in Fig. 1, however, the fusion cross-section of the D(d,p)T reaction separates from that of the D(d,n)$^3$He reaction, as the relative kinetic energy of reactants increases. In present magnetic confinement fusion devices, the DD fusion reaction between a neutral beam (NB) fast-ion and a thermal-ion is dominant. Therefore, in such cases, the tritium yields should be less than the neutron yields.

The experiment using deuterium gas began in 2017 [2–5] in the Large Helical Device (LHD). The LHD equips three negative ion-based neutral beam injection (N-NBI) systems [6], whose injection energy reaches $\sim$ 180 keV. If we consider the reaction between a stational deuteron and a 180 keV fast-deuteron, the fusion cross-section of the D(d,p)T branch is 10% less than that of the D(d,n)$^3$He branch from Fig. 1.

The investigation of the tritium inventory in fusion power plants is one of the most important issues for the studies of power plant design [7–9] because the tritium inventory affects the economic efficiency of the power plant, the safety assessment of tritium, the design of the tritium removal system, *etc*. Also in the LHD, an investigation of exhausted tritium [10] and remaining tritium in a vacuum vessel [11] have been performed.

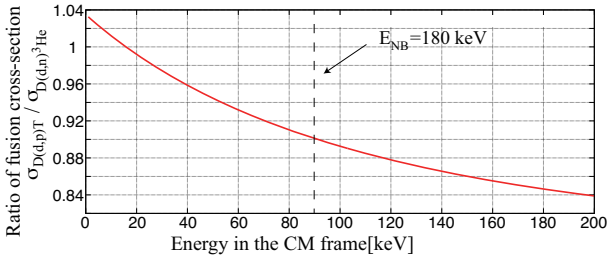


Fig. 1 The ratio of the fusion cross-section $\sigma_{D(d,p)T}/\sigma_{D(d,n)3He}$ against the kinetic energy in the center of mass (CM) frame is shown. The ratio of the fusion cross-section $\sigma_{D(d,p)T}/\sigma_{D(d,n)3He}$ between a stational deuteron and a 180 keV fast-deuteron is approximately 0.9, as shown by the dashed line. The parameters for the cross-section fit are given by Bosch and Hale [1].

In the first LHD deuterium experiment (19th campaign from March 2017 to August 2017), it was estimated that approximately 6.4 GBq of tritium was yielded and approximately 2.1 GBq of tritium was exhausted by the vacuum pumping system [12]. Therefore, it was evaluated that approximately 4.3 GBq of tritium remained in the vacuum vessel. However, the estimation of 6.4 GBq of tritium is based on the assumption that the amount of the tritium yields was equal to the amount of the neutron yields, which was measured by the neutron flux monitor [13–15] (NFM).

*author's e-mail: nuga.hideo@nifs.ac.jp*

*) This article is based on the presentation at the 30th International Toki Conference on Plasma and Fusion Research (ITC30).

It is expected that the actual tritium inventory in the vacuum vessel was less than 4.3GBq. The purpose of this study is to estimate the tritium yields by considering the velocity distribution function of fast-deuteron. Owing to the issue of the computation resources, a numerical estimation for the 22nd LHD experiment campaign has been performed in this paper.

The rest of this paper consists of the following. A summary of the deuterium experiment in the 22nd campaign is provided in section 2. A simulation method is introduced in section 3. Simulation results are shown in section 4 and a discussion about the result is in section 5. Section 6 concludes this paper.

## 2. Deuterium Experiment in the 22nd Campaign

A top view of the neutral beam injection (NBI) system in the LHD is shown in Fig. 2. Tangential NBs (NB#1 to NB#3) are a negative ion-based NBI (N-NBI) and perpendicular NBs (NB#4 and NB#5) are a positive ion-based NBI (P-NBI). The typical injection energy of N-NBIs is approximately $\lesssim$ 180 keV and that of P-NBIs is approximately $\lesssim$ 80 keV. Typical maximum values of the NB port-through power of each beam-line are $P_{\mathrm{NB}}^{\mathrm{port}} \lesssim 5$ MW for N-NBI and $P_{\mathrm{NB}}^{\mathrm{port}} \lesssim 10$ MW for P-NBI. In a usual operation, the beam port through power is limited that the shot integration of the beam power does not exceed 10 MJ in each beam-line.

According to a combination of beam ion species, the deuterium experiment in the 22nd experiment campaign can be classified into six phases, as shown in Table 1. In phase 0 (SN161168-SN161438) and phase 5 (SN166089-SN167808), the beam ion species of all beam-lines is hydrogen. In phase 1 (SN161439-SN162268) and phase 4 (SN164569-SN166088), the beam ion species of NB#1-NB#3 is hydrogen and that of NB#4 and NB#5 is the deuterium. In phase 2 (SN162269-SN162877), all beam-lines except NB#1 are deuterium beams. Only NB#1 is a hydrogen beam. In phase 3 (SN162878-SN164568), all beam-lines are deuterium beams. It is noted that the use of deuterium gas for the main plasma is permitted even in phase 0 and phase 5.

Figure 3 shows that neutron yields, which are measured by the NFM, per single discharge, during the deuterium gas experiment phase in the 22nd LHD experiment campaign. Values appearing at the top of Fig. 3 indicate the ratio of cumulative neutron yields, during each phase, to total neutron yields. From these values, it is found that the neutron yields in phase 0 and phase 5 can be negligible. In these two phases, there is no energetic deuteron because all beam-lines are hydrogen beams. Therefore, in the following sections, discharges in phase 1 to phase 4 are focused on. Most neutrons (87.5%) are yielded in phase 2 and phase 3 and the rest of the neutrons (12.5%) are yielded in phase 1 and phase 4. Due to higher injection energy of N-NBI, more neutrons are yielded in phase 2 and phase 3, rather than in phase 1 and phase 4.

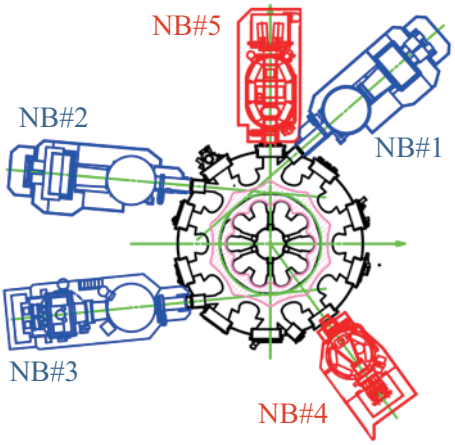


Fig. 2 The top view of the NBI system in the LHD is shown. NB#1-NB#3 are negative ion-based tangential beams and NB#4 and NB#5 are positive ion-based perpendicular beams. The typical injection energy of NB#1-NB#3 is $\sim$ 180 keV and that of NB#4 and NB#5 is $\sim$ 80 keV.

Table 1 The gas species of each beam-line is listed. The characters H and D indicate hydrogen and deuterium.

| | NB#1 | NB#2 | NB#3 | NB#4 | NB#5 |
|---|---|---|---|---|---|
| phase 0 | H | H | H | H | H |
| phase 1 | H | H | H | D | D |
| phase 2 | H | D | D | D | D |
| phase 3 | D | D | D | D | D |
| phase 4 | H | H | H | D | D |
| phase 5 | H | H | H | H | H |

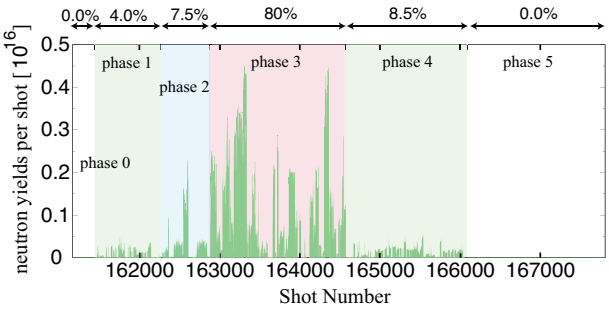


Fig. 3 Neutron yields per each discharge in the 22nd experiment campaign (SN161168-SN167808) against the shot number ID is shown.

## 3. Simulation Method

In the LHD and most of the present magnetic fusion devices, the deuterium-deuterium (DD) fusion reaction between a thermal deuteron and an energetic deuteron, so-called "beam-thermal" reaction, is dominant. Therefore, in the following simulations, we assume that all neutrons

are yielded by the beam-thermal fusion reaction. The influence of this assumption on the estimate of the tritium yields will be discussed in section 5.

The beam-thermal fusion reaction rate can be expressed as a reduced form:

$$\mathcal{R}_{\mathrm{b-th}} = n_D \int d\boldsymbol{v} \, \langle \sigma v \rangle_{\mathrm{b-th}} (v, T_D) f^{\mathrm{EP}}(\boldsymbol{v}), \tag{1}$$

where $n_D$ and $T_D$ indicate the bulk deuteron density and temperature and $f^{\mathrm{EP}}(\boldsymbol{v})$ indicates the velocity distribution function of the energetic deuteron. The approximate expression of beam-thermal reactivity, $\langle \sigma v \rangle_{\mathrm{b-th}} (v, T_D)$, is given by Mikkelsen [16] and the fitting parameters of the fusion cross-section are given by Bosch and Hale [1].

The flow of our simulation in TASK3D-a [17] consists of three steps. At first, three-dimensional magnetic equilibrium is calculated by VMEC code [18] to obtain an equilibrium magnetic configuration consistent with the mapping coordinate system [19].

Second, the birth profile of neutral beam fast ions is calculated by the FIT3D code [20–23] based on the obtained equilibrium and measured plasma parameters. In this step, after ionization of beam particles, their orbits are followed for a few tens of micro-seconds by MCNBI code, which is a component of FIT3D, to include the finite orbit width effect. Full, half, and one-third fractions of the beam injection energy for P-NBIs are assumed to be 0.78, 0.16, and 0.06, respectively. The electron density and temperature profiles measured by the Thomson scattering diagnostic system [24, 25] are taken as input.

Because the beam-thermal reactivity, $\langle \sigma v \rangle_{\mathrm{b-th}} (v, T_D)$, is independent of the velocity pitch angle of EPs, the pitch angle of EPs is not important for the estimation of the fusion reaction rate $\mathcal{R}_{\mathrm{b-th}}$. Therefore, at the third step, the velocity distribution function $f^{\mathrm{EP}}(\boldsymbol{v})$ is calculated by solving the fast-ion slowing down equation, which ignores the pitch angle scattering, in each beam-line. The fast-ion slowing down is simulated by CONV_FIT3D code [26], which is a two-dimensional (1-D in velocity space and 1-D in real space) code. Although CONV_FIT3D assumes that the fast-ions stay on the single magnetic flux surface until their slowing down process, finite orbit width effects such as birth profile broadening and prompt orbit loss are partially included, due to the orbit following simulation in the second step.

In the third step, the plasma is assumed to be pure deuterium plasma and the effective charge is assumed to be unity because the measurement of the density profile of impurity ions is not always available. This assumption causes an over-estimation of the beam-thermal fusion reaction rate $\mathcal{R}_{\mathrm{b-th}}$ because the deuteron density is usually less than the electron density in actual plasmas. However, this over-estimation of $\mathcal{R}_{\mathrm{b-th}}$, due to an over-estimation of $n_D$, is canceled in the ratio of tritium yielding rate to neutron emission rate, $S_t/S_n$, and in the ratio of tritium yields to neutron yields, $Y_t/Y_n$. Therefore, the ambiguity of the plasma effective charge is not important for the estimation of the tritium yields.

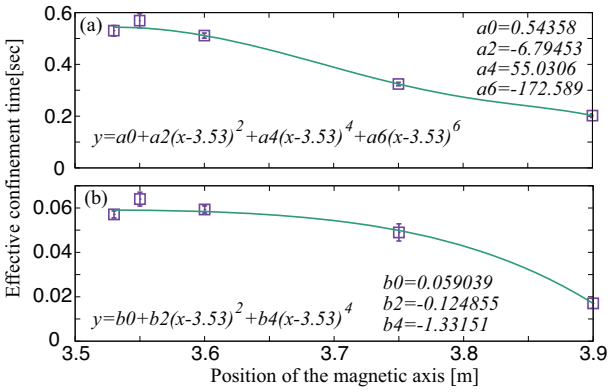


Fig. 4 The dependence of the effective confinement time $\tau_c^{\mathrm{eff}}$ for (a) tangential NBs and (b) perpendicular NBs on the position of the magnetic axis $R_{\mathrm{ax}}$ and its fitting curve are shown. The value of $\tau_c^{\mathrm{eff}}$ in $R_{\mathrm{ax}} < 3.53$ m is alternated by the value on $R_{\mathrm{ax}} = 3.53$ m.

It is also assumed that the plasma ion temperature is the same as the electron temperature $T_D = T_e$ in the third step because the measurement of the plasma ion temperature profile is not always available. Although the beam-thermal fusion reactivity $\langle \sigma v \rangle_{\mathrm{b-th}}$ depends on the deuteron temperature, as shown in equation (1), the reactivity is not sensitive to the deuteron temperature. Therefore, this assumption has no impact on the following simulation results.

The fast ion loss due to the transport in the third step is described by exponential decay in time with the time constant of the effective confinement time $\tau_c^{\mathrm{eff}}$. The values of $\tau_c^{\mathrm{eff}}$ applied in the following simulation are obtained in the LHD full field ($B_t \sim 2.75$ T) configuration [26]. The dependence of $\tau_c^{\mathrm{eff}}$ on the position of the magnetic axis $R_{\mathrm{ax}}$ is taken into account by the fitting curve shown in Fig. 4. According to our previous research [26], the fast-ion loss model with time constant $\tau_c^{\mathrm{eff}}$, which has no dependency on the plasma temperature and density, can reproduce the decay time of the neutron emission rate with a good agreement for $\tau_n^{\mathrm{cl}} < 0.4$ s plasmas. Here, $\tau_n^{\mathrm{cl}}$ is the $e$-folding time of the neutron decay time due to the classical fast-ion deceleration. The condition $\tau_n^{\mathrm{cl}} < 0.4$ s roughly corresponds to $n_e > 5 \times 10^{18}$ m$^{-3}$. In $\tau_n^{\mathrm{cl}} > 0.4$ plasmas, the values in Fig. 4 tends to be over-estimation.

For most of cases, the values of $\tau_c^{\mathrm{eff}}$ in Fig. 4 are over-estimation because the values are obtained in the strong magnetic field configuration, in the relatively high electron density plasmas, and in the Magneto-Hydro-Dynamics (MHD) quiescent discharges. The influence of this fast-ion loss model will be discussed in section 5.

In the 22nd LHD experiment campaign, ion cyclotron range of frequency (ICRF) heating has been performed. In the case of ICRF heating plasma without NBI heating, the neutron emission rate is $S_n \leq 10^{12}$ s$^{-1}$ [27]. This value of

the neutron emission rate is comparable to that of thermal-thermal fusion. Therefore, in the following simulations, the contribution of ICRF heating to neutron yields is not considered.

There is a fusion reaction between a fusion-born triton and a thermal deuteron. This reaction is the so-called "triton burn-up." This reaction also should be considered for the estimation of $Y_t$. The maximum value of the triton burn-up ratio achieved in the LHD is 0.45% [28]. For this result, the contribution of the triton burn-up to the total tritium yields can be ignorable.

## 4. Simulation Results

The simulation shown in section 3 has been performed for 4650 discharges in phase 1 to phase 4. Most simulations have been executed automatically by the AutoAna system [29].

The simulation results are shown in Fig. 5. Figure 5-(a) shows measured and simulated neutron yields per discharge. Figure 5-(b) shows measured cumulative neutron yields (solid curve), simulated cumulative neutron yields (dotted curve), and simulated cumulative tritium yields (dashed curve), respectively. Figure 5-(c) shows the ratio of the tritium yields to the neutron yields per discharge. Discharges, whose simulated neutron yields is less than $Y_n = 10^{12}$, are omitted in Fig. 5-(c). Figure 5-(d) shows the ratio of cumulative simulated tritium yields to cumulative simulated neutron yields. The solid curve in Fig. 5-(d) indicates the ratio of tritium yields, including the fast-ion loss shown in Fig. 4 and the dashed curve indicates that, excluding the fast-ion loss. In this simulation result, the neutron and tritium from the thermal-thermal fusion are not included. As noted in section 3, the simulated neutron yields are over-estimated in the whole discharges, as shown in Fig. 5-(a). The cumulative tritium yields are also over-estimated like the cumulative neutron yields, as shown in 5-(b).

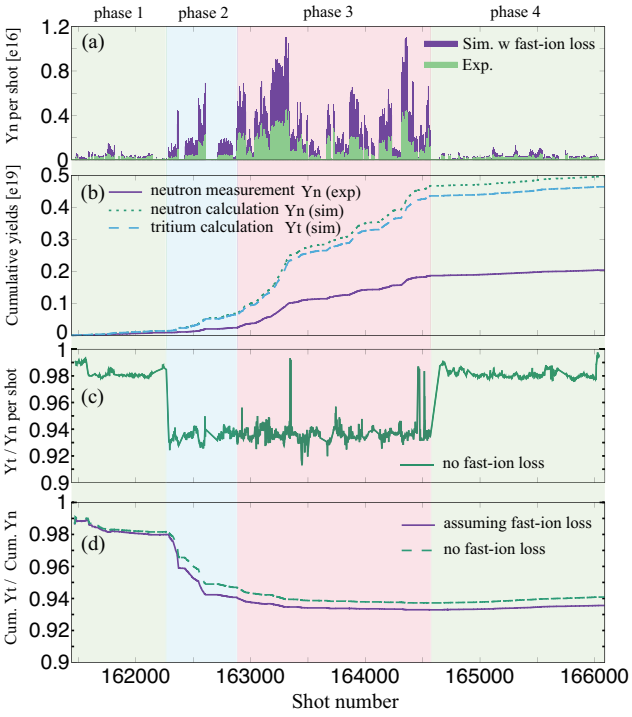


Fig. 5 (a) Measured and simulated neutron yields per discharge, (b) cumulative neutron yields (measured and simulated) and cumulative tritium yields (simulated) (c) the ratio of the tritium yields to the neutron yields per discharge, and (d) the ratio of the cumulative tritium yields to the cumulative neutron yields are shown.

From Fig. 5-(d), it is found that the ratio of the cumulative $Y_t/Y_n$ in phase 1 stays around 0.98. This is because only P-NBIs, whose injection energy is lower, rather than N-NBI, are deuterium beams in phase 1. From phase 2, the cumulative $Y_t/Y_n$ begins to separate from unity due to deuterium N-NBIs. Finally, the cumulative $Y_t/Y_n$ approaches 0.936 if the fast-ion loss is considered by the model shown in section 3.

## 5. Discussion

The simulation results in section 4 ignore the fusion reaction between fast-deuterons, so-called "beam-beam" fusion. In the LHD, as shown in Fig. 2, there are three N-NBIs. The direction of NB#1 and NB#3 is counter clockwise and the direction of NB#2 is clockwise. Therefore, the tangential balance injection by N-NBIs is available in the LHD. In such cases, the energy in the CM frame can reach 180 keV. According to Fig. 1, the ratio of the fusion cross-section can approach $\sigma_{\mathrm{D(d,p)T}}/\sigma_{\mathrm{D(d,n)3He}} \sim 0.85$ in the N-NBI balance injection. Therefore, the ignorance of the beam-beam fusion causes an over-estimation of $Y_t/Y_n$.

A more accurate estimation including beam-beam fusion costs much computation time rather than the present method because the relative velocity between fast-ions is required. It is difficult to perform such an accurate simulation for more than 4000 discharges. The inclusion of the beam-beam fusion component with the $Y_t/Y_n$ is future work.

Fast-ion loss is described by the model shown in section 3 in our simulation. The confinement time $\tau_c^{\mathrm{eff}}$ is obtained in the strong magnetic field configuration, the relatively higher electron density, and the MHD quiescent plasmas. Therefore, in actual cases, the fast-ion confinement time becomes shorter than the values used in our simulation. Because the fast-ion loss is described as exponential decay in time with the time constant $\tau_c^{\mathrm{eff}}$, particles immediately after injection are less reduced by $\tau_c^{\mathrm{eff}}$, and decelerated particles are much reduced by $\tau_c^{\mathrm{eff}}$. For this reason, a shorter confinement time tends to increase the averaged kinetic energy of non-thermal ions. For example, if the confinement time is $\tau_c^{\mathrm{eff}} \to 0$, $f^{\mathrm{EP}}$ becomes a delta function $f^{\mathrm{EP}}(v) \propto \delta(v - v_{\mathrm{inj}})$, where $v_{\mathrm{inj}}$ is the beam injection velocity. Therefore, the inclusion of the fast-ion loss reduces the value of $Y_t/Y_n$, as shown in Fig. 5-(d). For

these reasons, it can be considered that the value of the cumulative $Y_t/Y_n$ should be less than the present value due to the actual shorter confinement time.

According to the discussion in this section, it is considered that the actual value of the cumulative $Y_t/Y_n$ should be less than $Y_t/Y_n = 0.936$.

# 6. Conclusion

We have investigated the tritium yields, $Y_t$, during the 22nd LHD experiment campaign. Because the fusion cross-section of the D(d,p)T reaction becomes less than the fusion cross-section of the D(d,n)$^3$He reaction, as the relative kinetic energy increases, the tritium yields $Y_t$ should be less than the neutron yields $Y_n$ in the LHD deuterium experiment. Although it was reported that approximately 6.4 GBq of tritium was yielded and approximately 4.3 GBq of tritium remained in the vacuum vessel [10, 11] in the 19th LHD experiment campaign, the value of the remaining tritium should be less than 4.3 GBq by considering the fast-ion velocity distribution function. Therefore in this work, the ratio of the tritium yields to the neutron yields, $Y_t/Y_n$, during the 22nd LHD experiment campaign is numerically estimated for 4650 discharges by using integrated simulation code TASK3D-a.

The simulation results shown in Fig. 5 indicate that the ratio $Y_t/Y_n$ reaches 0.936. By considering the assumption applied in the simulation, it is found that the value $Y_t/Y_n = 0.936$ is still an over-estimation. The first reason is that the fast-ion confinement time used in the simulation is longer than the actual confinement time. In this paper, we have described the fast-ion loss by exponential decay with a time constant $\tau_c^{\mathrm{eff}}$. The value of $\tau_c^{\mathrm{eff}}$ is obtained empirically in the high magnetic field configuration and the MHD quiescent plasmas. Therefore in many cases, the actual fast-ion confinement time should be shorter than the value we used. A shorter confinement time tends to increase the averaged kinetic energy of energetic particles, because the decelerated particles are much reduced rather than the particles immediately after injection. For this reason, it is considered that the actual value of $Y_t/Y_n$ is less than $Y_t/Y_n = 0.936$ in this viewpoint.

The second reason is that we have ignored the fusion reaction between fast-ions, so-called "beam-beam" fusion. It is expected that the beam-beam fusion is not negligible in the LHD, due to the balance injection of tangential N-NBIs. From Fig. 1, the ratio of the fusion cross-section can be reduced down to $\sigma_{\mathrm{D(d,p)T}}/\sigma_{\mathrm{D(d,n)3He}} \sim 0.85$ in the N-NBI balance injection. Therefore, the ignorance of the beam-beam fusion causes the over-estimation of $Y_t/Y_n$. According to these two reasons, the value of $Y_t/Y_n$ during the 22nd LHD experiment campaign should be less than 0.936 in a real case.

A more accurate analysis, including the beam-beam fusion and the tritium yields estimate during the whole deuterium experiment campaign from 2017, are future works.

# Data Availability Statement

The LHD data can be accessed from the LHD data repository at https://www-lhd.nifs.ac.jp/pub/Repository_en.html


[1] H.-S. Bosch and G. Hale, Nucl. Fusion **32**, 611 (1992).
[2] Y. Takeiri, IEEE Trans. Plasma Sci. **46**, 2348 (2018).
[3] Y. Takeiri, IEEE Trans. Plasma Sci. **46**, 1141 (2018).
[4] M. Osakabe, M. Isobe, M. Tanaka *et al.*, IEEE Trans. Plasma Sci. **46**, 2324 (2018).
[5] M. Osakabe, Y. Takeiri, T. Morisaki *et al.*, Fusion Sci. Technol. **72**, 199 (2017).
[6] Y. Takeiri, O. Kaneko, K. Tsumori *et al.*, Fusion Sci. Technol. **58**, 482 (2010).
[7] H. Nakamura, S. Sakurai, S. Suzuki *et al.*, Fusion Eng. Des. **81**, 1339 (2006).
[8] I. Cristescu, I. Cristescu, L. Doerr *et al.*, Nucl. Fusion **47**, S458 (2007).
[9] T. Tanabe, Fusion Eng. Des. **87**, 722 (2012).
[10] M. Tanaka, N. Suzuki and H. Kato, J. Nucl. Sci. Technol. **57**, 1297 (2020).
[11] S. Masuzaki, T. Otsuka, K. Ogawa *et al.*, Physica Scripta **2020**, 014068 (2020).
[12] M. Tanaka, H. Kato, N. Suzuki *et al.*, Plasma Fusion Res. **15**, 1405062 (2020).
[13] M. Isobe, K. Ogawa, H. Miyake *et al.*, Rev. Sci. Instrum. **85**, 11E114 (2014).
[14] M. Isobe, K. Ogawa, T. Nishitani *et al.*, IEEE Trans. Plasma Sci. **46**, 2050 (2018).
[15] D. Ito, H. Yazawa, M. Tomitaka *et al.*, Plasma Fusion Res. **16**, 1405018 (2021).
[16] D. Mikkelsen, Nucl. Fusion **29**, 1113 (1989).
[17] M. Yokoyama, R. Seki, C. Suzuki *et al.*, Nucl. Fusion **57**, 126016 (2017).
[18] S.P. Hirshman and J. Whitson, Phys. Fluids **26**, 3553 (1983).
[19] C. Suzuki, K. Ida, Y. Suzuki *et al.*, Plasma Phys. Control. Fusion **55**, 014016 (2012).
[20] S. Murakami, N. Nakajima and M. Okamoto, Trans. Fusion Technol. **27**, 256 (1995).
[21] M. Sato, S. Murakami, A. Fukuyama *et al.*, Proc. 18th Int. Toki Conf, 2008.
[22] P. Vincenzi, T. Bolzonella, S. Murakami *et al.*, Plasma Phys. Control. Fusion **58**, 125008 (2016).
[23] R. Seki, K. Ogawa, M. Isobe *et al.*, Plasma Fusion Res. **14**, 3402126 (2019).
[24] K. Narihara, I. Yamada, H. Hayashi *et al.*, Rev. Sci. Instrum. **72**, 1122 (2001).
[25] I. Yamada, K. Narihara, H. Funaba *et al.*, Fusion Sci. Technol. **58**, 345 (2010).
[26] H. Nuga, R. Seki, K. Ogawa *et al.*, J. Plasma Phys. **86**, 815860306 (2020).
[27] R. Seki, S. Kamio, H. Kasahara *et al.*, Plasma Fusion Res. **15**, 1202088 (2020).
[28] K. Ogawa, M. Isobe, T. Nishitani *et al.*, Nucl. Fusion **59**, 076017 (2019).
[29] M. Emoto, C. Suzuki, M. Yokoyama *et al.*, Fusion Sci. Technol. **74**, 161 (2018).